ELSEVIER

Thin-Walled Structures 40 (2002) 1037–1049

THIN-WALLED STRUCTURES

www.elsevier.com/locate/tws

Reinversion of aluminium frustra

A.A.A. Alghamdi *

Department of Mechanical Engineering, King Abdulaziz University, P.O. Box 80204, Jeddah 21589, Saudi Arabia

Received 26 October 2001; received in revised form 18 May 2002; accepted 28 May 2002

Abstract

In this paper experimental study of plastic deformation of aluminum frusta when reinverted is presented. Effects of changing the angle of frustum as well as frustum wall thickness on the absorbed energy are investigated. The details of the experimental plastic inversion and reinversion are given. Obtained results show that it is possible to use the inverted aluminum frusta several times, thus they are reusable collapsible absorbers.

Keywords: Energy absorber; Frusta; Inversion; Reinversion

1. Introduction

The collapsible energy absorber is the device that converts the kinetic energy of a moving body into permanent plastic deformation in deformable solids. This conversion process depends on the shape of the absorber, material used, absorber arrangement, loading rate, loading pattern, and so on [1].

Energy absorbers are used mainly as crash protection devices. They are installed in critical areas, like automobile bumpers, to minimize the deceleration pulse during impact events. Knowing that the kinetic energy is constant, the function of the absorption device is to lower the impact force, and hence extend the dissipation period. Collapsible absorbers can be used inside automobile bumpers, along road

* Fax: 966-2-695-2193.
E-mail address: aljinaidi@hotmail.com (A.A.A. Alghamdi).

barriers, beneath armory surfaces, under lifts, surrounding nuclear reactors and as crash retards at harbors.

Collapsible energy absorbers can take several common shapes, such as circular tubes [2], multicorner columns [3], struts [4], frusta [4], and honeycomb cells [5]. Because of their common occurrence, axisymmetrical and circular shapes provide perhaps the widest range of all choices for use as absorbing elements, in addition to their favorable plastic behavior under axial forces. The selected absorber in this paper is capped-end aluminum frusta subjected to inversion load. Frusta are employed over a wide range of applications such as the nose cones of missiles and aircraft.

2. Thin-walled frusta

Thin-walled absorbers in the form of thin tubes have been of particular interest since the pioneering works of Alexander [2] in crushing thin tubes axially. Since then researchers have came up with different crushing mechanisms including, tube splitting [6], tube inversion [7], lateral indentation [8], tube nosing [9] and lateral flattening [10]. The study of deformation of tubular energy absorbers falls into two main categories, lateral, and axial loading. However, in comparing lateral crushing mode with axial, the specific absorption energy in axial mode is ten times that of the same tube when compressed laterally between flat plates. Investigations often lead to account for geometrical changes, interactions between modes of collapse, as well as strain hardening and strain rate effects.

Frustum is a truncated circular cone that can be seen in Fig. 1. One of the first studies in using frusta as energy absorbers was carried out by Postlethwaite and

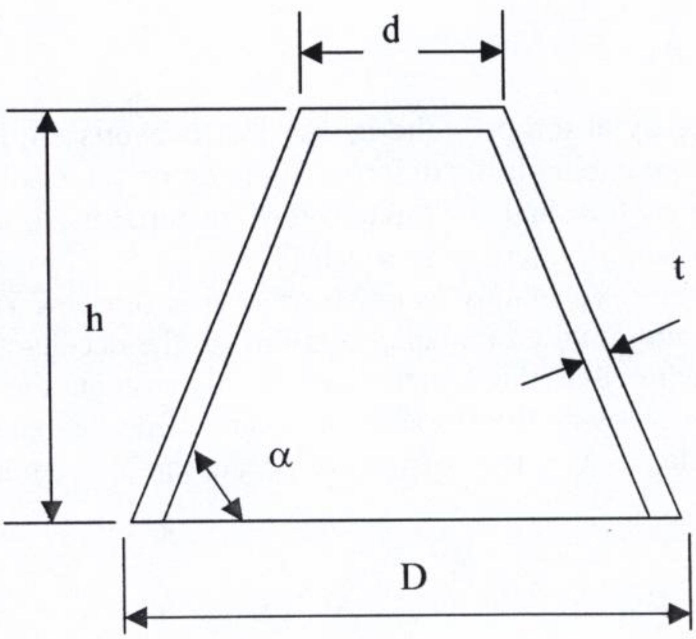

Fig. 1. Schematic drawing of the frustum.

Mills in 1970 [4]. They predicted the mean crushing force for concertina (symmetric) mode of deformation for frusta made of mild steel.

Mamalis and Johnson [11] investigated experimentally the crumbling of aluminum frusta when subjected to axial compression load under quasi-static conditions. Mamalis et al. [12] extended their experimental study to include mild steel at elevated strain rates. Mamalis et al. [13] proposed an extensible collapse analysis for predicting the mean crushing load for frusta crushed axially into concertina mode of deformation. Also, Mamalis et al. [14] developed a theoretical model for the average crushing force for frusta deformed axially into diamond (asymmetric) mode of deformation. In another paper, Mamalis et al. [15] modeled the progressive extensible collapse of frusta and gave a theoretical model that depicts the changes in peaks and troughs of the experimental load-displacement curves. Other studies related to axial crushing of frusta include crushing of PVC frusta of square cross-section [16], composite frusta [17,18], constrained frusta [19] and others [20,21].

All of the above studies deal with the axial crushing of frusta, however, Alghamdi [22] proposed inversion of frusta as an innovative mechanism of deformation. Details of the inversion of frusta have been investigated by Aljawi and Alghamdi [23] and deformation modes have been modeled using ABAQUS under static [24] and dynamic [25] loadings.

In this paper the inverted frusta are used again as energy absorbers in an attempt to maximize the energy absorbed per unit mass that can be considered as an acceptable measure of the success of an absorber. Although inversion of frustum is a plastic deformation process, it produces an inverted frustum with a slight permanent deformation that can be used again and again.

3. Results and discussion

A number of frusta, featuring different thicknesses and angles were inverted and reinverted up to failure. The program involved the use of 15 different sizes of aluminum frusta (ten different angles and five different thicknesses) in reinversion tests. Tests were conducted using 10-ton Instron Universal Testing Machine (UTM). A special jig for inversion was manufactured and utilized. The jig consisted of an inversion rod (to be held by the upper jaw of the UTM) and a base cylinder working as a seat for the frustum while resting on the lower jaw. Table 1 lists the dimensions of the frusta used in the reinversion tests where D is the large diameter, d is the small diameter, α is the angle of the frustum, h is the height, m is the mass and t is the thickness, see Fig. 1.

The inversion tests were carried out first for 46 capped-end aluminum frusta made by a spinning process. Fig. 2 shows a photograph of the specimens after the first inversion, details of the inversion process can be found in [25].

Selected specimens featuring different angles and thicknesses were chosen for reinversion tests. The program started by testing specimens 30102–30302 that have a constant angle ($\alpha = 30°$) but different thicknesses, varying from 1.01 to 3.05 mm. Then specimens with different angles were reinverted. Table 2 lists the details of

Table 1
Specimens used in the reinversion tests

SP	D (mm)	d (mm)	α (deg)	h (mm)	m (g)	t (mm)
30102	72.04	24.52	30	15.8	12.212	1.01
30152	72.26	25.56	30	15.5	16.95	1.43
30202	72.94	26.32	30	16.4	24.464	2.04
30252	73	27.64	30	15.6	29.951	2.57
30302	71.22	28	30	16.74	34.205	3.05
35102	69.74	23.22	35	16.22	11.841	1.02
35152	69.56	24.14	35	17.3	15.944	1.38
40152	73	23.46	40	22.22	18.057	1.32
45152	71.78	23.8	45	25.72	19.37	1.36
50152	71.88	23.26	50	30.54	19.737	1.24
55152	72.7	23.9	55	36.04	22.647	1.27
60152	72.46	24.08	60	44	23.551	1.14
65152	72.48	23.22	65	54.58	26.237	1.08
70152	72.49	23.2	70	68.86	28.552	0.97
75152	72.56	23.2	75	94.42	37.543	0.96

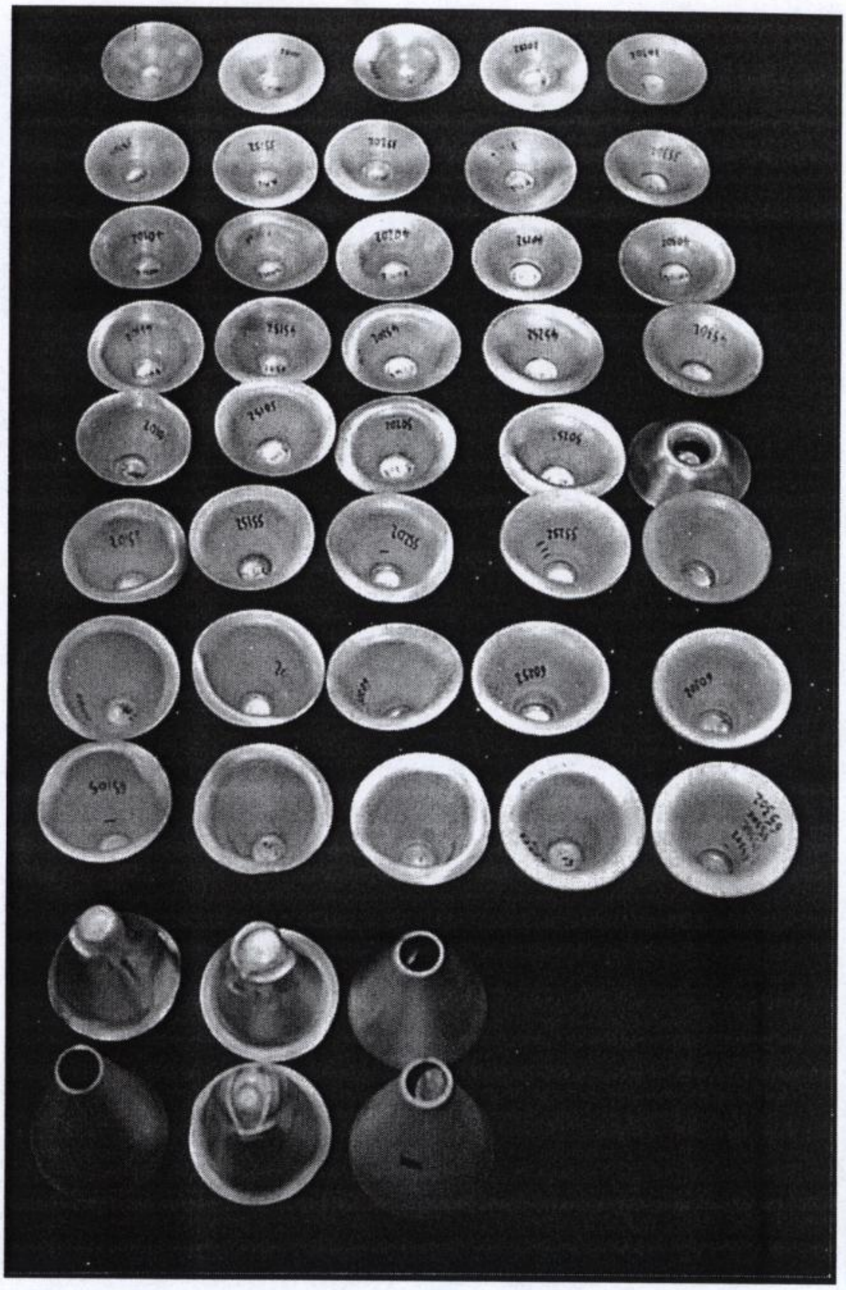

Fig. 2. Spun aluminum specimens after the first inversion.

the experimental work that includes the inversion stage, energy absorbed, measured by the area under force-displacement curve, and specific energy.

Reinversion load-displacement curves are similar to each other and good representative examples are shown in Fig. 3 for Specimen 50152. This specimen sustains four inversions. In the first inversion, the frustum passes through a number of stages. The load rises from the origin to the instability point. Up to 90% of this point the deformation is recoverable, i.e., elastic and beyond which plastic behavior sets in. The second stage is the zone of incubation, or the zone of inversion preparation, where an extensible mode of deformation is observed and the load decreases to a minimum value. Inversion then proceeds towards the larger (lower) end of the frustum, with a linear increase in the load. The increase in the inversion force is attributed

Table 2
Details of the experimental work

SN	SP	t (mm)	α (deg)	m (g)	Inversion	Energy (J)	Specific energy (J/g)
1	30102	1.01	30	12.212	1	16.97901	1.390354705
2	30102	1.01	30	12.212	2	20.28266	1.660879388
3	30102	1.01	30	12.212	3	19.73406	1.615956555
4	30102	1.01	30	12.212	4	17.19879	1.408351284
5	30152	1.43	30	16.95	1	26.10718	1.54024666
6	30152	1.43	30	16.95	2	24.54913	1.44832634
7	30152	1.43	30	16.95	3	32.98926	1.94626915
8	30152	1.43	30	16.95	4	34.61843	2.042385472
9	30152	1.43	30	16.95	5	50.60674	2.985648094
10	30152	1.43	30	16.95	6	23.29213	1.37416677
11	30202	2.04	30	24.464	1	51.73379	2.114690497
12	30202	2.04	30	24.464	2	49.94086	2.041402074
13	30202	2.04	30	24.464	3	71.97848	2.942220262
14	30202	2.04	30	24.464	4	65.63016	2.682724012
15	30202	2.04	30	24.464	5	56.35857	2.303734706
16	30252	2.57	30	29.951	1	62.53395	2.087875303
17	30252	2.57	30	29.951	2	61.23654	2.044557527
18	30252	2.57	30	29.951	3	101.4664	3.387746573
19	30252	2.57	30	29.951	4	88.66666	2.960390508
20	30302	3.05	30	34.205	1	106.3545	3.109325268
21	30302	3.05	30	34.205	2	104.9818	3.069195877
22	30302	3.05	30	34.205	3	147.38	4.308726082
23	30302	3.05	30	34.205	4	80.98411	2.367610225
28	35152	1.38	35	15.944	1	42.74374	2.6808667
29	35152	1.38	35	15.944	2	36.58267	2.294447486
30	35152	1.38	35	15.944	3	48.92187	3.068356431
31	35152	1.38	35	15.944	4	13.71086	0.859938682
32	40152	1.32	40	18.057	1	55.3885	3.067425374
33	40152	1.32	40	18.057	2	48.51798	2.686934809
34	40152	1.32	40	18.057	3	59.38934	3.288992724

(continued on next page)

Table 2 (*continued*)

SN	SP	t (mm)	α (deg)	m (g)	Inversion	Energy (J)	Specific energy (J/g)
35	40152	1.32	40	18.057	4	25.78766	1.42812564
36	45152	1.36	45	19.37	1	80.46033	4.153863279
37	45152	1.36	45	19.37	2	73.28531	3.783443949
38	45152	1.36	45	19.37	3	99.40395	5.131850911
39	45152	1.36	45	19.37	4	44.21323	2.282561951
40	50152	1.24	50	19.737	1	107.6929	5.456398589
41	50152	1.24	50	19.737	2	111.2978	5.639045066
42	50152	1.24	50	19.737	3	136.2252	6.902019641
43	50152	1.24	50	19.737	4	28.26595	1.432130179
44	55152	1.27	55	22.647	1	150.7276	6.655519965
45	55152	1.27	55	22.647	2	158.3272	6.991090455
46	55152	1.27	55	22.647	3	213.8274	9.441752821
47	55152	1.27	55	22.647	4	34.82098	1.537553732
48	60152	1.14	60	23.551	1	181.9451	7.72557866
49	60152	1.14	60	23.551	2	203.0836	8.623140591
50	60152	1.14	60	23.551	3	248.3384	10.544709
51	60152	1.14	60	23.551	4	195.6342	8.306830507
52	65152	1.08	65	26.237	1	248.5201	9.472123042
53	65152	1.08	65	26.237	2	248.509	9.471701865
54	65152	1.08	65	26.237	3	261.1639	9.954031044
55	65152	1.08	65	26.237	4	17.84874	0.680288905
56	70152	0.97	70	28.552	1	289.2773	10.13159349
57	70152	0.97	70	28.552	2	130.1843	4.559550916
58	75152	0.96	75	37.543	1	408.283	10.87507657
59	75152	0.96	75	37.543	2	177.1576	4.71879233

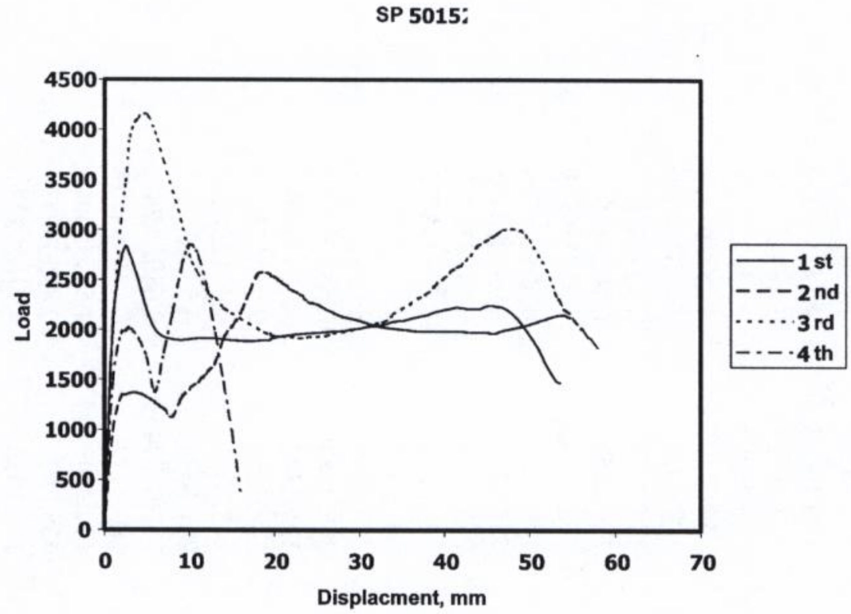

Fig. 3. The first 4 inversion curves for specimen 50152.

to the progressive increase in the volume of the deformation zone with increasing diameter/thickness ratio. The second maximum point in the solid curve signals the termination of the inversion zone and the start of bending of the free large end of the frustum. Thus the inversion mode changes into flattening mode where the undeformed lower part of the frustum has the shape of Belleville spring. The free end of the frustum is flattened parallel to the shoulder of the jig base. The energy absorbed recorded experimentally through first inversion is 107.7 J, whereas the calculated specific energy is 5.456 J/g for this specimen.

In the second inversion, the specimen is removed from the holder and upturned upside down so that the small capped-end faces the inversion rod. The second inversion is similar to the first one except the delay in the maximum instability point due to the massive plastic deformation applied to the upper capped-end of the frustum in the first inversion (Fig. 3). The curve follows, to some extent, the first inversion curve with total absorbed energy equal to 111.3 J, and specific energy equal to 5.639 J/g (Table 2).

The third inversion curve is very similar to the first one but with higher instability point and larger absorbed energy, 136.2 J, and specific energy, 6.902 J/g. The increase in the absorbed energy is a result of the cold-work strengthening done to the specimen in the previous inversions. In the fourth inversion, the test was stopped because the lower end of the frustum became so deformed that it passed through the holder. Fig. 4 shows photographs of Specimen 55152 after the second and the third inversions, and final shapes of Specimens 30102, 30152, 30202, 30252 and 30302.

It is very clear that the absorbed energy increases by the increase in the number of inversions (N), thus Figs. 5 and 6 are given to show the effect of angle of frustum (α) and wall thickness (t) on the number of inversions (N), respectively. It can be seen from Fig. 5 that the number of inversions decreases with the increase in the

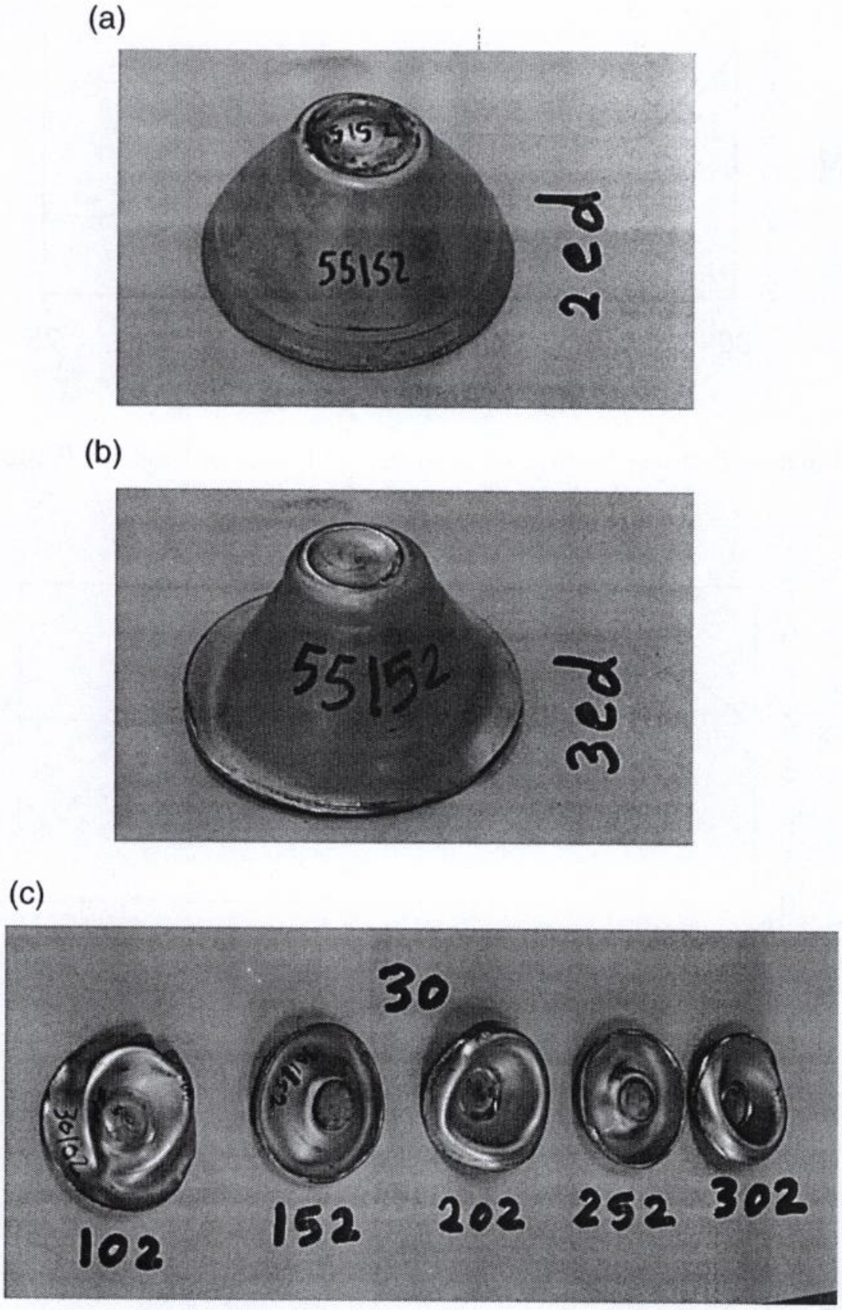

Fig. 4. Specimens after inversion. a) Specimen 55152 after the second inversion, b) Specimen 55152 after the third inversion, c) Final shapes of specimens 30102, 30152, 30202, 30252 and 30302.

angle of frustum. In other words, the possibility of inversion decreases due to the difficulty of inversion process with large angle. For $\alpha = 90°$ frustum becomes a tube and inversion of a tube is limited to one inversion per tube [7]. At the other extreme, frusta with small angles are very close to Belleville springs where the elastic response dominates the inversion process, thus, theoretically, it can be inverted an infinite number of times. For the thickness change, it seems to be that there is some optimum thickness, for the given geometry, at which the number of inversions is maximum. This value is approximately $t = 1.5$ mm.

The effects of the angle of frustum and wall thickness on the total absorbed energy are shown in Figs. 7 and 8. Generally, one can say that the total absorbed energy

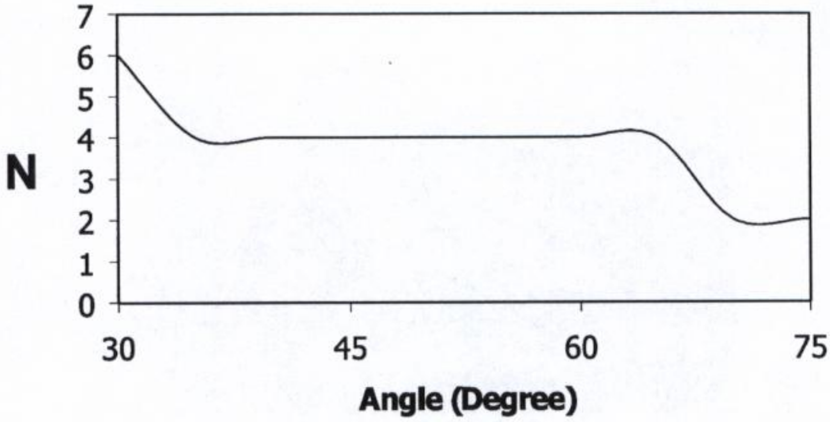

Fig. 5. Relation Between Number of Inversions (N) and The Angle of Frustum (α).

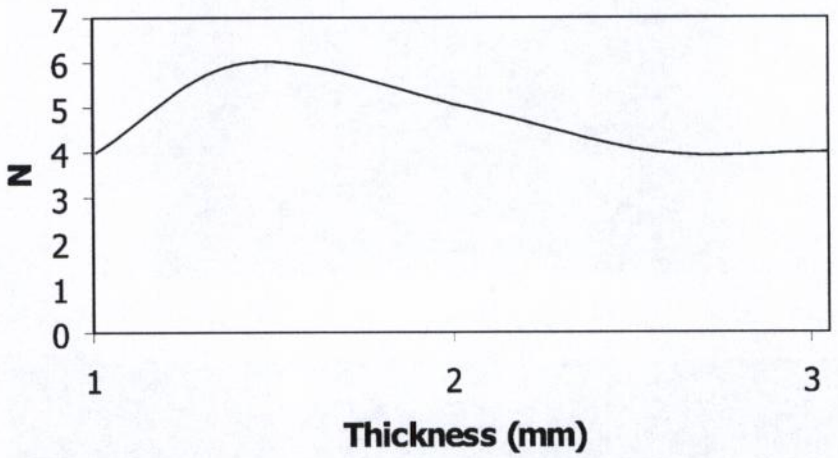

Fig. 6. Relation Between number of inversions (N) and frustum wall thickness (t).

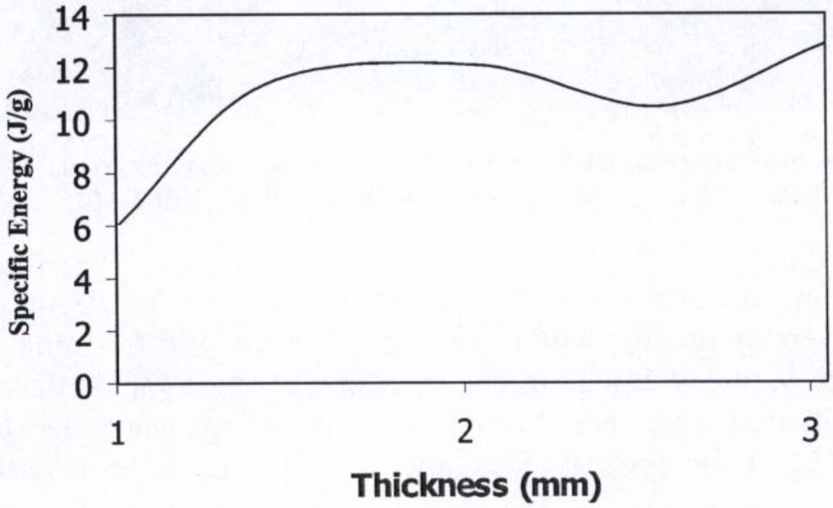

Fig. 7. Effect of wall thickness on energy absorbed.

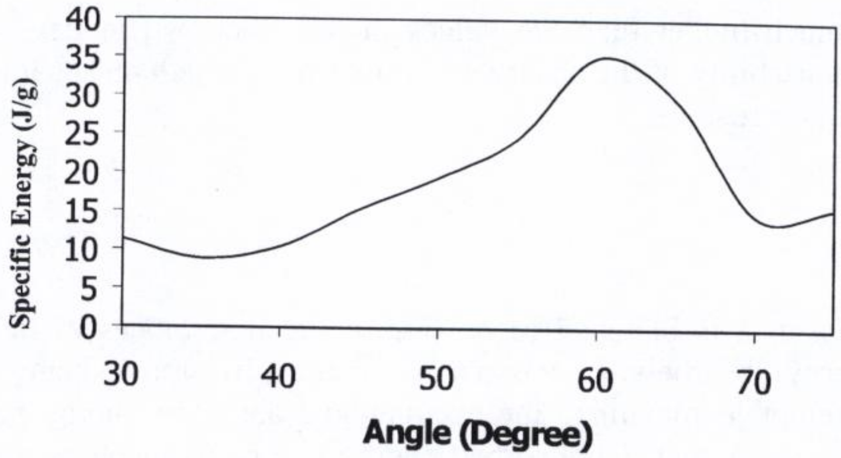

Fig. 8. Effect of angle of frustum on energy absorbed.

increases with the increase in wall thickness. This is a more accurate measure than the number of inversions (N) that measures the reusability of the absorber. The effect of the angle is very clear. As expected, the accumulated absorbed energy increases with the increase in the angle of frustum, and the absorbed energy attains some maximum value at $\alpha = 60°$.

Fig. 9 illustrates a comparison between the reinversion of frusta with other modes of deformation such as inversion and crushing. The plot gives the experimental specific energy vs the angle of frustum for the three modes of deformation. The circle points depict the inversion mode as reported by Aljawi et al. [25], the triangle points present the crushing mode as reported by Alghamdi et al. [26], the square points mimic the crushing mode, as predicted by El-Sobky et al. [19], and finally the star points show the reinversion mode. It can be seen that absorbed energy in the reinver-

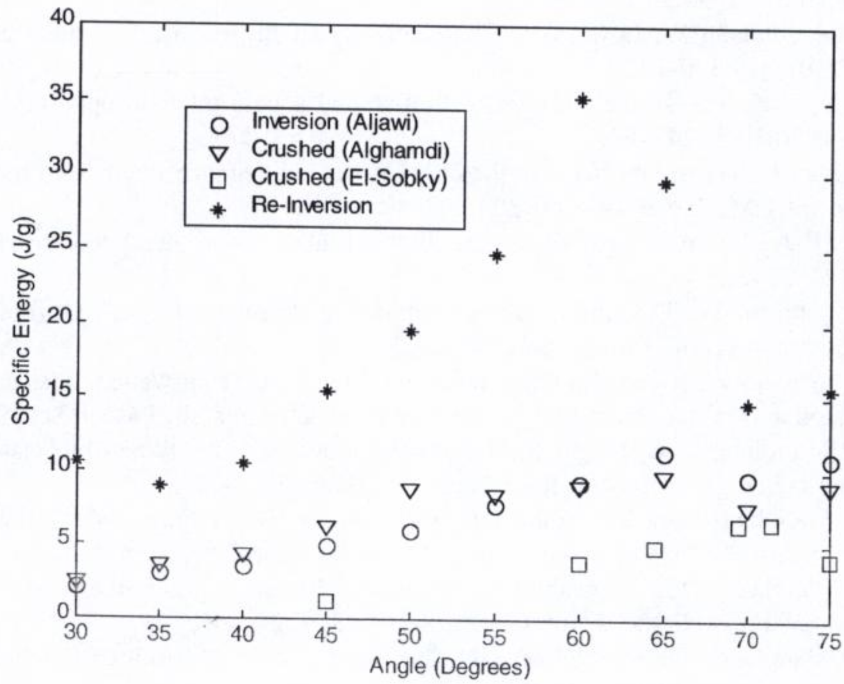

Fig. 9. Absorbed energy density for crushing, inversion and reinversion.

sion mode is much higher than the values in the other two modes. Again this is attributed to the usability of the absorber several times, which means it is not disposable after the first crushing.

4. Conclusions

Inversion of frusta is believed to be one of the best modes of deformation of collapsible energy absorbers. In this paper, inverted frustum is being used several times in an attempt to maximize the accumulated absorbed energy per unit mass. Obtained results show that the absorbed energy can be as much as three times the energy absorbed by crushing. This signals the possibility of using frusta several times in inversion mode, and hence it is not disposable after the first time of usage like crushing of tubes or frusta.

References

[1] Alghamdi AAA. Collapsible impact energy absorbers: an overview. Thin-Walled Struct 2001;39:189–213.
[2] Alexander JM. An approximate analysis of the collapse of thin cylindrical shells under axial loading. Quart J Mech Appl Math 1960;13:10–5.
[3] Reddy TY, Al-Hassani STS. Axial crushing of wood-filled square metal tubes. Int J Mech Sci 1993;35:231–46.
[4] Postlethwaite HE, Mills B. Use of collapsible structural elements as impact isolators with special reference to automotive applications. J Strain Anal 1970;5:58–73.
[5] Wu E, Jiang W-S. Axial crush of metallic honeycombs. Int J Impact Eng 1997;19(5/6):439–56.
[6] Lu G, Ong LS, Wang B, Ng HW. An experimental study on tearing energy in splitting square metal tubes. Int J Mech Sci 1994;36:1087–97.
[7] Al-Hassani STS, Johnson W, Lowe WT. Characteristics of inversion tubes under axial loading. J Mech Eng Sci 1972;14:370–81.
[8] Gupta NK, Sinha SK. Transverse collapse of thin-walled square tubes in opposed loadings. Thin-Walled Struct 1990;10(3):247–62.
[9] Reid SR, Harrigan JJ. Transient effects in the quasi-static and dynamic internal inversion and nosing of metal tubes. Int J Mech Sci 1998;40(2/3):263–80.
[10] Wu L, Carney III JF. Initial collapse of braced elliptical tubes under lateral compression. Int J Mech Sci 1997;39(9):1023–36.
[11] Mamalis AG, Johnson W. The quasi-static crumpling of thin-walled circular cylinders and frusta under axial compression. Int J Mech Sci 1983;25:713–32.
[12] Mamalis AG, Johnson W, Viegelahn GL. The crumbling of steel thin-walled tubes and frusta under axial compression at elevated strain-rate: some experimental results. Int J Mech Sci 1984;26:537–47.
[13] Mamalis AG, Manolakos DE, Saigal S, Viegelahn G, Johnson W. Extensible plastic collapse of thin-wall frusta as energy absorbers. Int J Mech Sci 1986;28:219–29.
[14] Mamalis AG, Manolakos DE, Viegelahn GL, Vaxevanidis NM, Johnson W. On the inextensional axial collapse of thin PVC conical shells. Int J Mech Sci 1986;28:323–35.
[15] Mamalis AG, Manolakos DE, Viegelahn GL, Johnson W. The modeling of the progressive extensible plastic collapse of thin-wall shells. Int J Mech Sci 1988;30:249–61.
[16] Mamalis AG, Manolakos DE, Viegelhan GL. The axial crushing of thin PVC tubes and frusta of square cross-section. Int J Impact Eng 1989;8(3):241–64.
[17] Mamalis AG, Manolakos DE, Demosthenous GA, Ioannidis MB. Analytical modelling of the static

and dynamic axial collapse of thin-walled fiberglass composite conical shells. Int J Impact Eng 1997;19(5/6):477–92.

[18] Mamalis AG, Manolakos DE, Demosthenous GA, Ioannidis MB. Energy absorption capability of fibreglass composite square frusta subjected to static and dynamic axial collapse. Thin-Walled Struct 1996;25(4):269–95.

[19] El-Sobky H, Singace AA, Petsios M. Mode of collapse and energy absorption characteristics of constrained frusta under axial impact loading. Int J Mech Scis 2001;43:743–57.

[20] Gupta NK, Abbas H. Axisymmetric axial crushing of thin frusta. Thin-Walled Struct 2000;36:169–79.

[21] Chryssanthopoulos MK, Poggi C. Collapse strength of unstiffened conical shells under axial compression. J Const Steel Res 2001;57:165–84.

[22] Alghamdi AAA. Design of simple collapsible energy absorber. Master of Science Thesis, College of Engineering, King Abdulaziz University, Jeddah, Saudi Arabia, 1991.

[23] Aljawi AAN, Alghamdi AAA. Investigation of axially compressed frusta as impact energy absorbers. In: Gaul L, Brebbia AA, editors. Computational methods in contact mechanics IV. Southampton: WIT Press; 1999. p. 431–43.

[24] Aljawi AAN, Alghamdi AAA. Inversion of frusta as impact energy absorbers. In: Hassan MF, Megahed SM, editors. Current advances in mechanical design and production VII. New York: Pergamon; 2000. p. 511–9.

[25] Aljawi AAN, Alghamdi AAA, Abu-Mansour TMN. Details of experimental investigation and finite element analysis of the inversion of capped end frusta as impact energy absorbers. Int J Impact Eng, Accepted, 2002.

[26] Alghamdi AAA, Aljawi AAN, Abu-Mansour TMN. Modes of axial collapse of unconstrained capped frusta. Int J Mech Eng, Accepted, 2002.